A Morphological Model for the Solvent-Enhanced Conductivity of PEDOT:PSS Thin Films

ARTICLE *in* ADVANCED FUNCTIONAL MATERIALS · MARCH 2008

Impact Factor: 11.81 · DOI: 10.1002/adfm.200700796

3 AUTHORS, INCLUDING:

Alexandre Nardes
National Renewable Energy Laboratory
38 PUBLICATIONS **1,176** CITATIONS
SEE PROFILE

Martijn Kemerink
Linköping University
149 PUBLICATIONS **3,970** CITATIONS
SEE PROFILE

ADVANCED FUNCTIONAL MATERIALS

FULL PAPER

DOI: 10.1002/adfm.200700796

A Morphological Model for the Solvent-Enhanced Conductivity of PEDOT:PSS Thin Films**

By *Alexandre Mantovani Nardes, René A. J. Janssen,* and *Martijn Kemerink**

The well-known enhanced conductivity of poly(3,4-ethylenedioxythiophene):poly(4-styrenesulfonate) (PEDOT:PSS) thin films that is obtained by addition of high-boiling solvents like sorbitol to the aqueous dispersion used for film deposition is shown to be associated with a rearrangement of PEDOT-rich clusters into elongated domains, as evidenced from STM and AFM. Consistently, temperature dependent conductivity measurements for sorbitol-treated films reveal that charge transport occurs via quasi 1D variable range hopping (VRH), in contrast to 3D VRH for untreated PEDOT:PSS films. The typical hopping distance of 60–90 nm, extracted from the conductivity measurements is consistent with hopping between the 30–40 nm sized grains observed with scanning probe microscopy.

1. Introduction

The performance of (opto)electronic devices based on organic and polymer materials as active layer or electrodes is found to be closely related to mesoscopic (dis)order and other morphological properties of the active materials.[1–4] For that reason, it is crucial to understand the effects of molecular arrangement on the electronic properties of organic materials and organic-based devices. A detailed comprehension on how charges move through the material is probably the best feedback to assist in the aforementioned development of novel devices. Hence, considerable efforts have been made to improve and understand the charge transport characteristics of these materials.[5] Temperature dependent conductivity measurements are likely the most direct way to experimentally study the mechanism of charge transport in organic conjugated systems and the results can directly be compared with predictions of theoretical models.[6,7] However, a common problem in charge transport studies on organic materials is a lack of detailed knowledge of the morphology.

A good example of this problem is the well-known but poorly understood highly conducting state of poly(3,4-ethylenedioxythiophene):poly(4-styrenesulfonate) PEDOT:PSS, obtained by the addition of high boiling solvents or polar compounds to the water-borne dispersion.[8–13]. Technologically, highly conducting PEDOT:PSS opens opportunities to replace the well-known but expensive inorganic indium tin oxide (ITO) as anode in optoelectronic devices, like organic photovoltaic cells[14,15] and organic light emitting diodes,[16–19] and forms a good candidate for electrodes for field-effect transistors[20] and circuits in general.[21]

The origin of this conductivity increase has been tentatively explained in literature and related to changes on (*i*) a nanoscopic level such as increase in interchain interactions, conformational changes in PEDOT chains,[22] and screening effects between polymer and dopant due to the polar solvent, or to changes on (*ii*) a mesocopic level leading to the formation of larger particles with concomitant reduction of the PPS shell and increased hopping between particles.[23–26] However no strong consensus among the explanations has been found. In this work, we use scanning probe techniques to actually visualize the film morphology of both pristine and sorbitol-treated films and relate the observed solvent-induced ordering to the change in conduction mechanism as derived from temperature dependent transport measurements.

Typically, the temperature dependent conductivity in doped organic materials like PEDOT:PSS can be described in the framework of variable range hopping (VRH) as:

$$\sigma = \sigma_0 \exp\left[-\left(\frac{T_0}{T}\right)^{\alpha}\right] \quad (1)$$

In Equation (1), σ_0 is the conductivity at infinite temperature, T_0 is the characteristic temperature and α the exponent that in standard VRH theory is equal to $1/(1+D)$, where D is dimensionality of the system. Assuming that the density of the states near the Fermi level $N(E_F)$ is either constant or varies smoothly with energy, Mott obtained $\alpha = ¼$ in three dimensions (3D). Straightforward application of Equation (1) to 1D systems turned out to be problematic because of the presence of 'blocking sites' in infinitely long 1D chains. However, Shante et al.[27] have shown that the conductivity of 'real' systems, consisting of a large number of parallel 1D chains of finite length, can be described by Equation (1). Later

[*] Dr. M. Kemerink, A. M. Nardes, Prof. R. A. J. Janssen
Molecular Materials and Nanosystems
Department of Applied Physics
Eindhoven University of Technology
PO Box 513, 5600 MB Eindhoven (The Netherlands)
E-mail: m.kemerink@tue.nl

[**] We thank Dr. Albert J. J. M. van Breemen of TNO Science and Industry and Dr. Margreet de Kok of Philips for providing materials and discussions. A. M. Nardes acknowledges the Alβan Program (the European Union Programme of High Level Scholarships for Latin America, ID#E03D19439BR) for the financial support.

it was shown that for both 2D and 3D VRH systems at (very) low temperatures $\alpha = ½$ can also result from long-range electron-electron interactions which give rise to a Coulomb gap in $N(E_F)$. Finally, $\alpha = ½$ has also been interpreted in terms of a charging-energy-limited tunneling model.[28–30] In this model, the energy barrier the tunneling charge has to overcome is assumed to result from the capacitive coupling between the metallic particle and its surrounding, rather than from energetic disorder. However, in this model proportionality between (insulating) shell thickness and core diameter of the metallic particles is required, for which, in the case of PEDOT:PSS, no experimental indications are found.

Previous studies concerned with the effect of addition of high-boiling solvents to the solution used for spin coating on the charge transport properties of the resulting PEDOT:PSS films have shown that the conductivity can be enhanced by several orders of magnitude, depending on the solvent. Kim et al. found that $\sigma(T)$ of PEDOT:PSS deposited from pure H_2O followed a quasi 1D VRH model, while that of high conductive PEDOT:PSS deposited with organic solvents followed a power law $\sigma(T) \sim T^{-\alpha}$, with α varying from 0.54 to 1.2. Ouyang et al.[31] and Ashizawa et al.[32] have also described their results for ethylene glycol treated PEDOT:PSS using the 1D VRH model. In contrast, Crispin et al. concluded that upon the addition of diethylene glycol a three-dimensional conducting network is formed, which in principle should lead to $\alpha = ¼$. Their X-ray photoelectron spectroscopy (XPS) studies indicated that sorbitol and diethylene glycol induce a morphology change at the surface of PEDOT:PSS and these results were interpreted as a segregation of the excess PSS, however no clear connection was made between the topography of the film and XPS measurements.[33] Timpanaro et al. have shown with scanning tunneling microscopy that the addition of sorbitol leads to an increase in the apparent size of the PEDOT-rich particles, which is associated with the increase of conductivity. Thus, the morphology change in the PEDOT:PSS appears to be another plausible mechanism to explain the high conductivity of PEDOT:PSS. In conclusion, the conductivity enhancement is well established, but the responsible mechanism has been controversial.

The present paper aims to resolve this problem and describes the temperature dependence of the DC conductivity of sorbitol-treated PEDOT:PSS, both in low and moderate electric fields, in combination with a morphology analysis by scanning probe microscope (SPM) techniques. To allow direct comparison, some previously published data[34,35] for the non-treated material are included. The transition from 3D to quasi-1D VRH conduction that is found upon addition of sorbitol appears to be due to a rearrangement of PEDOT-rich particles into elongated and aligned clusters in which the charge transport takes place. The characteristic hopping distance matches well with the observed size of the PEDOT particles. Finally, the conductivity enhancement is attributed to an increased effective localization length.

2. Results

2.1. Charge Transport

The temperature dependent conductivity of the pristine PEDOT:PSS, Figure 1(a) and three different sorbitol films, Figure 1(b) were measured between 77 and 300 K. The data can be very well fitted to the variable range hopping model (Equation (1)) as demonstrated in Figure 1. In fact, the correct exponent α in Equation (1) was determined as the α value at which the correlation coefficient R of the fit in Figure 1 reached a maximum. These fits were sufficiently sharp and the best α values, using this approach, have more than 96% of accuracy for all samples. The insets of Figure 1 show R of the fits of Equation (1) to the measured conductivity plotted versus the exponent α. The optimal α values (Table 1) for sorbitol treated PEDOT:PSS are very close to ½, which we interpret as indicative of quasi 1D VRH. Alternative interpretations of this finding are discussed at the end of this section. In contrast, the pristine material exhibited 3D VRH behavior, as concluded from the value of ¼ found for α, see Figure 1(a). Hence, sorbitol treatment has resulted in a transition from 3D VRH to quasi 1D VRH.

Once the transport mechanism of sorbitol-treaded material is identified as quasi 1D VRH, the other parameters in

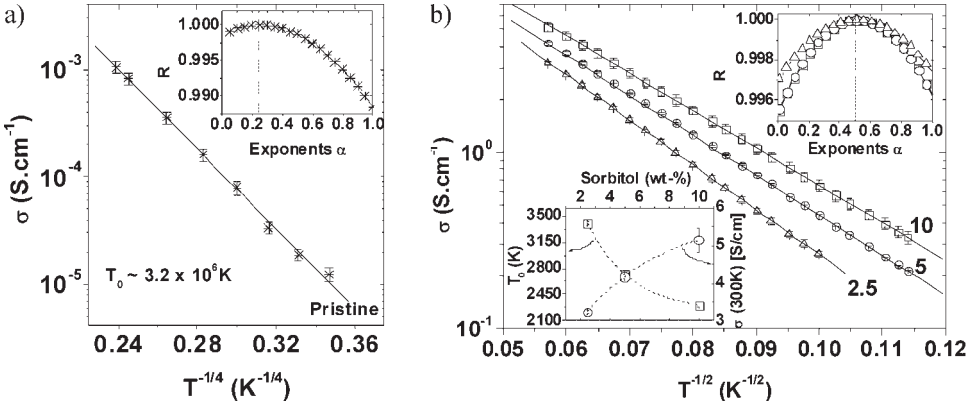

Figure 1. Temperature dependence of the conductivity for (a) pristine PEDOT:PSS sample and (b) PEDOT:PSS samples treated with (△) 2.5 wt%, (○) 5 wt% and (□) 10 wt% of sorbitol concentration added to the aqueous dispersion used for spin coating of the films. Straight lines are fits to Equation (1). Upper right inset: analysis of the exponent α for the whole temperature range, i.e. the correlation coefficient R of the fit of Equation (1) to the data in the main panel plotted versus α. The vertical dashed line represent $\alpha = ¼$ in (a) and ½ in (b). Lower left inset of (b): evolution of T_0 and σ at 300 K as a function of sorbitol concentration, the dashed lines serves to guide the eye. The values of these parameters are also shown in Table 1.

ADVANCED FUNCTIONAL MATERIALS

Table 1. Parameters describing the electrical conduction in pristine and sorbitol-treated PEDOT:PSS thin films.

	Pristine	2.5 wt%	5 wt%	10 wt%
Hopping transport	3D-VRH	1D-VRH	1D-VRH	1D-VRH
σ at 300 K (S cm^{-1})	$(1.1 \pm 0.1) \times 10^{-3}$	3.24 ± 0.06	4.18 ± 0.07	5.2 ± 0.3
α (77 K–307 K)	0.25 ± 0.1	0.52 ± 0.01	0.53 ± 0.02	0.52 ± 0.01
T_0 (K)	$(3.2 \pm 0.1) \times 10^6$	3406 ± 26	2720 ± 27	2314 ± 27
σ_0 (S cm^{-1})	24.7 ± 1.3	91.3 ± 1.3	83.3 ± 1.4	81.7 ± 1.5
$N(E_F)$ (eV · cm^3)$^{-1}$	$(1.4 \pm 0.2) \times 10^{17}$	$(1.9 \pm 0.4) \times 10^{18}$	n.d.	$(1.8 \pm 0.3) \pm 10^{18}$
ξ' (nm)	8.2 ± 0.5	33 ± 2	n.d.	44 ± 3
L (nm)	30–40	60–80	n.d.	65–95

Equation (1) can also be discussed. The slopes of the curves in Figure 1 represent the quantity $-T_0^{1/2}$, where T_0 is given by:

$$T_0 = \frac{4}{k_B N(E_F) \xi'} \quad (2)$$

Here, ξ' is the effective localization length, $N(E_F)$ is the density of (localized) states at the Fermi level, k_B is Boltzmann's constant. The systematic variation of T_0 and σ at 300 K as a function of sorbitol concentration is shown in the lower left inset of Figure 1(b). T_0 drops and σ (300 K) increases by addition of sorbitol to the aqueous PEDOT:PSS dispersion up to 10 wt%. Coincidently, they both vary by a similar fraction. Common explanations for this behavior suggest a lower energy barrier between the hopping sites and/or a longer localization length of the charge and/or an increasing of $N(E_F)$. However, authors have only looked at the variation of T_0, which indeed depends on $N(E_F)$ and ξ', see Equation (2), but no quantitative analysis has been made so far. In order to clarify this issue, we measured the electric field dependence of the conductivity, which allows one to extract the characteristic length scales of the hopping process.

As the electric field is increased, deviations from Ohmic behavior become evident. In Figure 2, the electric field dependence of the conductivity is plotted at different temperatures for 0, 2.5, and 10 wt% of sorbitol. The electric-field dependent conductivity $\sigma(F)$ for hopping in disordered systems in moderate electric fields F is of the general form:[36,37]

$$\sigma(T,F) = \sigma(T,0) \exp\left(c \frac{eFL}{k_B T}\right) \quad (3)$$

Here, eFL is the energy that electrons can pick-up from the electric field in one hop which, at intermediate fields, is comparable to the activation energy of the dominant or characteristic hop. In this term, L is the characteristic hopping length and e the electronic charge. The prefactor c accounts for the fact that not all critical hops are in the direction of the applied field, and different authors predict different values for c, depending on the assumptions made. For 3D VRH, Pollak and Riess have found $c = 0.17$, which is used in the analysis of the data in Figure 2(a). In the following analysis of the quasi 1D VRH data we will use Equation (3) with $c = 1$, mainly because of the absence of an applicable theory for non-Ohmic quasi 1D VRH. As a result, the extracted hopping lengths should be considered a lower limit to the real value.

At each temperature in Figure 2, the data are fitted quite well by Equation (3) at low to moderate electric field. Deviations from straight lines in Figure 2(b, c) indicate the onset of another conduction mechanism at high electric field, which is beyond the scope of the present work. The origin of the large

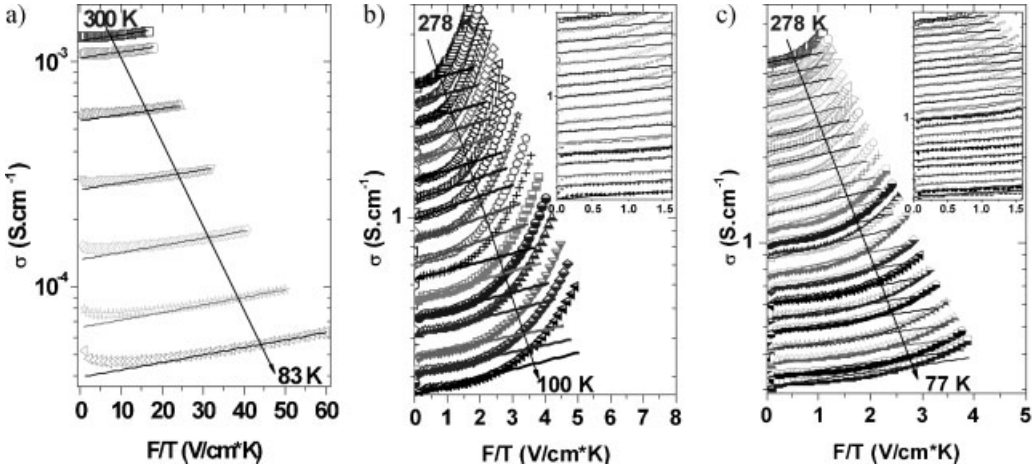

Figure 2. Conductivity as a function of F/T for PEDOT:PSS thin films at different temperatures: (a) pristine, (b) 2.5 wt% and (c) 10 wt%. Solid lines are fits to Equation (3) and the insets of (b) and (c) shows the same data restricted to low/moderated electric fields.

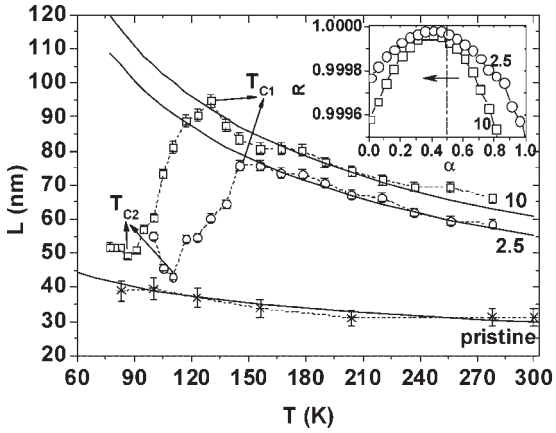

Figure 3. Temperature dependence of the characteristic hopping length for PEDOT:PSS thin films: (*) pristine film, and films with (○) 2.5 wt% and (□) 10 wt% of sorbitol added to the aqueous dispersion used for depositing the layers. The dashed lines connect the data points, the solid lines are fits to Equation (4) for sorbitol-treated samples and to $L \propto (T_0/T)^{\frac{1}{4}}$ for pristine. The inset shows the analysis of the power exponent α in Equation (1) for temperatures below T_{C1}, i.e. the correlation coefficient R to the fit of Equation (1) is plotted versus α. A vertical dashed line at $\alpha = \frac{1}{2}$, clearly shows the shift of the best-fitting value of α to lower values, in this case $\alpha_{2.5\ wt\%} = 0.40 \pm 0.02$ and $\alpha_{10\ wt\%} = 0.39 \pm 0.03$.

positive differential conductivity at very low (<0.1 V cm^{-1} K^{-1}) fields for sorbitol-treated films are unclear at present, and the corresponding data points were excluded from the fitting procedure. As the temperature is changed, the slope of the lines through the data in Figure 2 also changes. The temperature dependency of the hopping length $L(T)$ extracted from the slopes of Figure 2 is shown in Figure 3. For both the 2.5 and 10 wt% samples, the hopping length increases with decreasing temperature and reaches a maximum at a critical temperature T_{C1}, 145 K and 130 K for 2.5 and 10 wt% samples, respectively. After T_{C1}, a sudden decrease in the hopping length is observed and the values of L reach a second critical temperature T_{C2} after which they seem to saturate or even start rising again. In contrast, this behavior is not observed for the pristine material. The inset of Figure 3 shows the analysis of the power exponent α in Equation (1) for temperatures below T_{C1}. Although we previously found an excellent correspondence with $\alpha = ½$ for the whole temperature range in Figure 1, α is found to be less than ½ for the specific range below T_{C1}. We shall further discuss this behavior in the discussion section.

The characteristic hopping length in 1D VRH is expected to vary as $T^{-½}$ according to:

$$L(T) = \frac{\xi'}{2}\left(\frac{T_0}{T}\right)^{½} \tag{4}$$

which is used to extract ξ' from the measured samples in Figure 3. Good agreement between Equation (4) and the data in Figure 3 is obtained in the range where L continuously increases, and the extracted ξ' values are shown in Table 1. They are found to be about a factor 5 larger than that of pristine samples (8.2 nm). Next, from T_0 and ξ' we have calculated the 1D density of states $N(E_F)$ using Equation (2), and found 4.2×10^6 and 4.6×10^6 eV^{-1}cm^{-1} for 2.5 and 10 wt%, respectively. By using the width (30–40 nm, respectively) and thickness (6–7 nm) of the 1D channels (see next section) these numbers can be transformed into an estimate for the 3D density of states, see Table 1.

While the results in Figure 3 corroborate our identification of quasi-1D VRH as the transport mechanism around room temperature, the behavior at $T < T_{C1}$, requires an alternative interpretation. The Efros-Shklovskii or Coulomb gap model should be relevant only at low temperatures, i.e. the thermal energy should be smaller than the width of the Coulomb gap, i.e. $k_B T < \Delta$. Ignoring any anisotropy, Δ can be estimated as $\Delta \approx \sqrt{N(E_F)e^6 / (4\pi\varepsilon_0\varepsilon_r)^3}$. By taking $N(E_F) \sim 10^{18}$ eV^{-1}cm^{-3} and assuming $\varepsilon_r = 3$, Δ is roughly 10 meV or 120 K, which is very close to the observed values of T_{C1}. Hence, the discontinuity in $L(T)$ at T_{C1} can tentatively be attributed to a transition to another transport regime, governed by the opening of a Coulomb gap. At T_{C2} the transition appears to have completed. Depending on the details of the system, the associated temperature exponent α can theoretically expected to be ½ or $^2/_5$.[38] The experimentally extracted values for α below T_{C1} closely match the latter number; it is however not clear whether the theory in ref. [38] can directly be applied to the present granular system. In addition, the remaining temperature range below T_{C2} is too small to extract a value for α with any accuracy and we refrain from a further analysis of the low temperature data.

Finally, it is interesting to point out that Samitsu et al. found the same temperature dependence of the conductivity for 1D PEDOT fibers, and interpreted this in terms of 1D VRH.[39] This corroborates our notion that in the type of material system investigated here, an elongated morphology can indeed result in (quasi) 1D VRH.

2.2. Morphology

The interpretation of the charge transport data of sorbitol-treated PEDOT:PSS thin films in terms of a quasi-1D VRH model is striking in view of the fact that charge transport in pristine films of the same material is governed by 3D VRH, i.e. $\alpha = ¼$. This transition can however be readily understood from changes in the film morphology as seen by low-current STM, see Figure 4. Clearly, for the sample made without adding sorbitol (referred to as 0 wt%), the 20–25 nm sized PEDOT-rich particles are (almost) randomly distributed. Upon adding sorbitol to the aqueous dispersions used for spin coating, these particles arrange spontaneously along lines that, for the image size shown, all run in a preferential direction. It seems logical to assume that the particles are more strongly coupled, i.e. are separated by a thinner PSS barrier, along these lines than perpendicular to these lines. This assumption directly explains the quasi-1D behavior of the sorbitol treated samples. Actually, this morphology seems to be a perfect example of

ADVANCED FUNCTIONAL MATERIALS

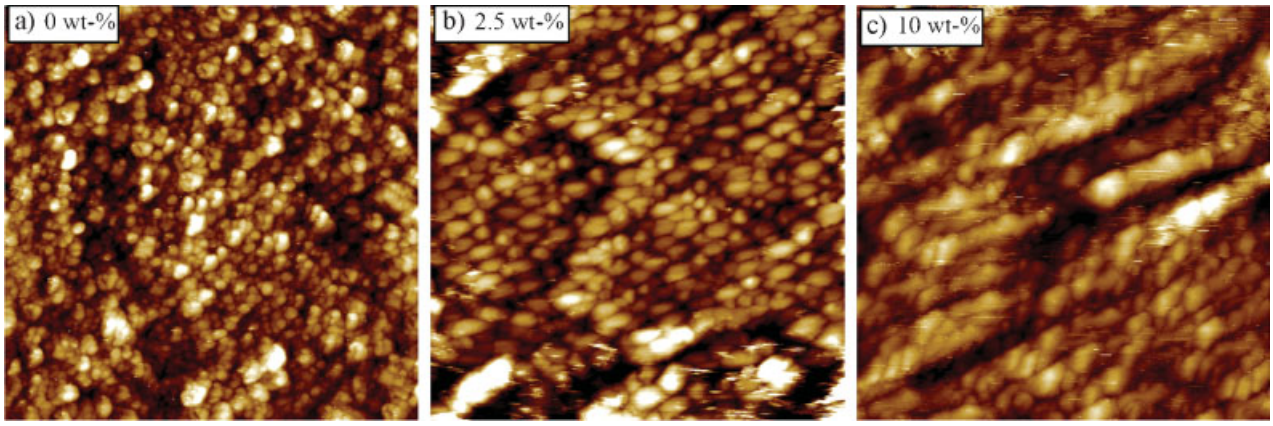

Figure 4. Topographic STM images of PEDOT:PSS spin coated on ITO with different sorbitol concentration in the aqueous dispersion: (*a*) 0 wt% (pristine) [bias: 2.3 V; $I_{tunneling}$: 20 pA], (*b*) 2.5 wt% [bias: 0.1 V; $I_{tunneling}$: 10 pA], and (*c*) 10 wt% [bias: 0.5 V; $I_{tunneling}$: 0.5 pA]. All images were captured in areas of 500×500 nm^2 and vertical scale of 10 nm. The 20-40 nm sized bright objects and the thin depressions are interpreted as PEDOT-rich particles and separating PSS barriers, respectively.

'a large number of parallel chains of finite length' that was considered in ref. [27].

Despite the strong particle alignment in sorbitol-enhanced films and the fact that such alignment is found everywhere on the sample, no preferential orientation direction could be observed on length scales above ca. 1 μm. Due to the random orientation of these ordered domains, the macroscopic in-plane conductivity is most likely isotropic.[40] Since the typical domain size is at least one order of magnitude bigger than the characteristic hopping length, one may anticipate that the macroscopic conductivity is limited by the intra-domain conduction, leading to the observed quasi-1D behavior. Conversely, if inter-domain hopping would be the rate-limiting process, it is hard to see how the observed 1D VRH could result.

Another effect of the addition of sorbitol is an increase in size of the PEDOT-rich particles. Going from the pristine PEDOT:PSS sample, Figure 4(a), to 10 wt% sorbitol, Figure 4(c), the particle diameter increases from 20–25 nm to about 40 nm in average. Qualitatively, an increased particle size may be expected to result in a reduced density of states. However, $N(E_F)$ of the present samples is about an order of magnitude higher than the value of 1.4×10^{17} eV^{-1}cm^{-3} found for pristine films. We tentatively attribute this increase to a narrowing of the density of states resulting from reduced disorder in the sorbitol treated films. In addition, batch-to-batch variations, which can amount up to a factor two or so in T_0, may play a role.

The size of the PEDOT-rich particles is fully consistent with the observed, rather large, hopping length L in Figure 3. This implies that the conduction in sorbitol-treated PEDOT:PSS, like in the pristine material, takes place by hopping of charge carriers between PEDOT-rich particles, rather than between single molecular sites.

To complete the morphological picture, we performed cross-sectional phase-imaging AFM (X-AFM) on cryogenically cleaved sorbitol treated films, see Figure 5. This technique was previously shown to allow the visualization of PEDOT-rich and PSS-rich regions because of differences in viscoelastic properties. The absence of strong correlation between panels (a) and (b) of Figure 5 excludes the possibility that the phase contrast is due to cross talk with the topography. In Figure 5 it can be seen that in the vertical direction the sorbitol treated film consists of flattened dark areas, which we interpret as the PEDOT-rich domains, separated by quasi continuous bright areas, interpreted as PSS lamellas. The typical in-plane size of the PEDOT-rich particles is of the same order as that of the spherical objects in Figure 4(b), consistent with the interpretation of these as the PEDOT-rich clusters. This lamellar morphology is very similar to the one observed in our previous work for pristine films. Apparently, the sorbitol-facilitated reorganization of PEDOT and PSS does not significantly affect the phase separation in the vertical direction.

3. Discussion

Comparing the values of the effective localization length ξ' for sorbitol samples (30–45 nm, see Table 1) and that found for pristine material (8 nm, ref.), we observe an increase of about a factor 4–5. In a granular material the use of an effective localization length, rather than of the normal one, reflects the fact that the wave function only picks up a significant 'tunneling action' in the separating barriers, i.e. in the PSS. Hence, ξ' and ξ are related via $\xi' = \xi(d+s)/s$ with d and s the particle diameter and barrier thickness, respectively.[41] The observed increase of ξ' upon including sorbitol in film formation is most likely due to a decrease in s, since d increases only slightly. The decrease in s is consistent with a reduction of the in-plane hopping barriers that mainly consist of PSS due to the plasticizing action of sorbitol. Moreover, a reduced inter-particle tunneling barrier

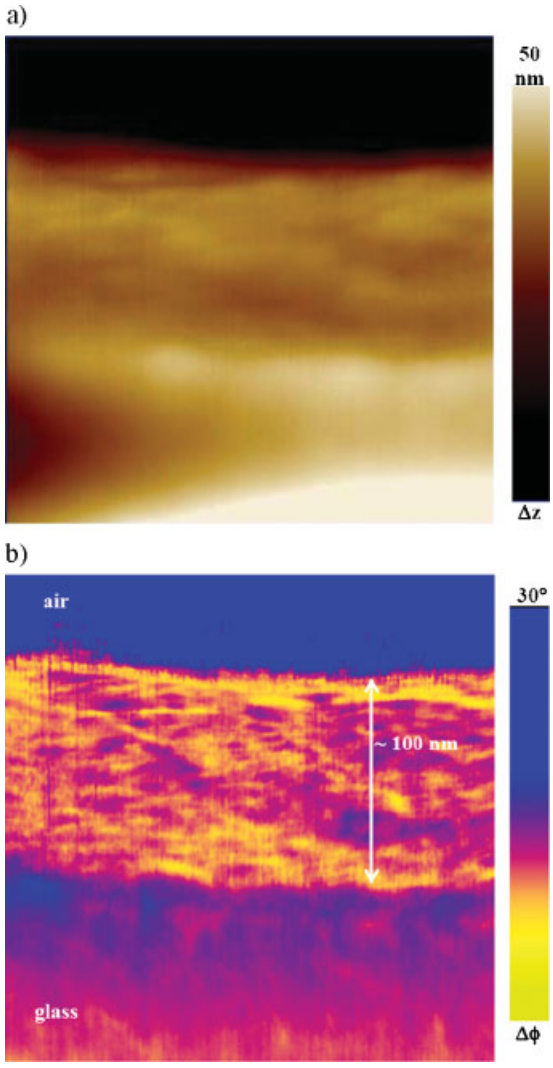

Figure 5. 250×250 nm^2 (a) topographic and (b) cross-sectional AFM phase image of cleaved PEDOT:PSS deposited on glass from am aqueous dispersion containing 2.5 wt% sorbitol. Bright and dark areas in the phase image (b) of the PEDOT:PSS film are interpreted as PSS lamellas and PEDOT-rich particles, respectively [35].

width s explains the large increase in conductivity upon (increasing) sorbitol treatment.

Another interesting issue is why sorbitol treatment causes the observed ordering. In our previous work, we found that on a fraction of the investigated positions of pristine films, an organization that is very similar to what is observed here for sorbitol treated material is observed. However, for pristine materials, this is the exception, whereas for sorbitol treated material, the ordering is always observed. Hence, the conductivity of the pristine material will be dominated by the least conducting, i.e. the most disordered, areas. However, the occurrence of ordered regions in pristine material strongly suggests that this material has an inherent tendency to order that may be frustrated by the rapid drying during spin coating. Upon annealing the film in the presence of a high boiling solvent, this tendency may become fully expressed.

The data presented here show a large difference between the pristine material on one hand and on the sorbitol treated material on the other. Clearly, increasing the sorbitol loading of the casting dispersion above 2.5 wt% has only a minimal effect, in line with earlier observations by Huang et al., who found that the transition from 'low' to 'high' conductivity occurs between 0.1 and 1 wt% sorbitol.[26] A similar observation was made by Crispin et al. for diethylene glycol.[18]

4. Conclusions

We have studied the conductivity of PEDOT:PSS thin films deposited by spin coating from aqueous dispersions containing a high-boiling solvent (sorbitol). We found that the well-known conductivity enhancement by several orders of magnitude is accompanied by a transition from 3D variable range hopping to quasi-1D VRH. Using scanning probe microscopy, the latter effect could be explained by a sorbitol-induced self-organization of the PEDOT-rich grains into 1D aggregates between which hopping of charge carriers takes place. Although these aggregates are aligned within (sub) micrometer sized domains, these domains seem to have no preferential orientation, i.e. no macroscopic in-plane anisotropy is present. The typical hopping distance of 60–90 nm, which is extracted from non-Ohmic transport, matches well with hopping between 30–40 nm sized grains. Combining these results, the sorbitol-induced conductivity increase could be attributed to a decrease in thickness of the PSS barrier separating the PEDOT-rich grains.

5. Experimental

The substrates (3×3 cm^2 bare or ITO-covered sodalime glass) were first cleaned with soap and subsequently sonicated in baths of acetone and isopropyl alcohol for 20 min. each and rinsed with deionized water after each process. Any residual organic contaminations were removed using a 30 min. UV-ozone treatment (UV-Ozone Photoreactor, PR-100, Ultraviolet Products).

Four gold electrodes (1×6 mm with 1 mm spacing) were evaporated on top of cleaned glass substrates using a shadow mask. Prior to evaporation of 95 nm of gold, 5 nm of Cr were evaporated in order to improve adhesion.

To the PEDOT:PSS aqueous dispersion, purchased from H. C. Starck by the trade name of Baytron P VP Al 4083, 2.5, 5.0 and 10 wt% of D-sorbitol 97% (Sigma-Aldrich) were added and stirred for at least 24 h at room temperature. Solutions were filtered using a 5 μm filter and deposited in air by spin coating, which resulted in 90–100 nm thick films as measured by a profilometer (Alpha-step 200, Tencor Instruments). Then, samples were transferred into a glove box (O_2 and $H_2O < 1$ ppm) and annealed on a hot plate at 200 °C for 2 min to remove water and most of the sorbitol. After cutting the desired sample from the substrate, it was placed inside a cryostat (Oxford Instruments), evacuated to 10^{-5} mbar and brought to the desired temperature in the 77–300 K range. Temperature control was provided by an Oxford ITC 601 Temperature Controller that maintained temperature stability within ±0.1 K. Electrical measurements were performed by either a semiconductor parameter analyzer (Agilent model 4156C) or via Keithley 2410 source meter connected to a PC. For all temperature-dependent measurements the electrical connections were made inside the glove box, so the measured samples never experienced contact with air after bake-out. From a comparison of

ADVANCED FUNCTIONAL MATERIALS

2- and 4-terminal measurements the contact resistance was found to be negligible for all our samples. Moreover, control experiments were performed to assure that our results are not affected by ionic currents.

Scanning tunneling microscopy (STM) experiments were performed with a Veeco/Digital Instruments MultiMode equipped with a low current STM unit, driven by a NanoScope IV controller. For the STM measurements, freshly cut Pt-Ir tips were used and the experiments were conducted in air on PEDOT:PSS films deposited on glass covered with ITO. Tapping mode cross-sectional atomic force microscopy (X-AFM) experiments were measured with a Veeco/Digital Instruments Dimension 3100, driven by a NanoScope IIIA controller. For the X-AFM measurements, $3 \times 3\ cm^2$ PEDOT:PSS thin films on glass were frozen to liquid nitrogen temperature and then broken into small pieces. The tips (PPP-NCHR from NanoSensors) used in this experiment had a spring constant $k \approx 20\ N\ m^{-1}$.

Received: July 18, 2007
Revised: November 09, 2007

[1] F. P. Wenzl, P. Pachler, C. Suess, A. Haase, E. J. W. List, P. Poelt, D. Somitsch, P. Knoll, U. Scherf, G. Leising, *Adv. Funct. Mater.* **2004**, *14*, 441.
[2] B. J. Schwartz, *Ann. Rev. Phys. Chem.* **2003**, *54*, 141.
[3] R. Kline, R. M. McGehee, *Polym. Rev.* **2006**, *46*, 27.
[4] H. Hoppe, N. S. Sariciftci, *J. Mater. Chem.* **2006**, *16*, 45.
[5] V. I. Arkhipov, I. I. Fishchuk, A. Kadashchuk, H. Bässler, in *Photophysics of Molecular Materials: From Single Molecules to Single Crystals*, (Ed: G. Lanzani), Wiley-VCH, **2006**, p. 261–366.
[6] N. Mott, E. A. Davis, in *Electronic Processes in Non-Crystalline Materials*, Clarendon Press, Oxford **1979**.
[7] B. I. Shklovskii, A. L. Efros, in *Electronic Properties of Disordered Semiconductors*, Springer, Berlin **1984**.
[8] F. Jonas, A. Karbach, B. Muys, E. van Thillo, R. Wehrmann, A. Elschner, R. Dujardin, European Patent EP 686662, **1995**.
[9] L. A. A. Pettersson, S. Ghosh, O. Inganäs, *Organ. Electron.* **2002**, *3*, 143.
[10] J. Y. Kim, J. H. Jung, D. E. Lee, J. Joo, *Synth. Met.* **2002**, *126*, 311.
[11] F. J. Touwslager, N. P. Willard, D. M. de Leeuw, *Synth. Met.* **2003**, *135–136*, 53.
[12] F. Louwet, L. Groenendaal, J. Dhaen, J. Manca, J. Van Luppen, E. Verdonck, L. Leenders, *Synth. Met.* **2003**, *135–136*, 115.
[13] M. Döbbelin, R. Marcilla, M. Salsamendi, C. Pozo-Gonzalo, P. M. Carrasco, J. A. Pomposo, D. Mecerreyes, *Chem. Mater.* **2007**, *19*, 2147.
[14] F. Zhang, M. Johansson, M. R. Andersson, J. C. Hummelen, O. Inganäs, *Adv. Mater.* **2002**, *14*, 662.
[15] H. J. Snaith, H. Kenrick, M. Chiesa, R. H. Friend, *Polymer* **2005**, *46*, 2573.
[16] A. J. Mäkinen, I. G. Hill, R. Shashidhar, N. Nikolov, Z. H. Kafafi, *Appl. Phys. Lett.* **2001**, *79*, 557.
[17] W. H. Kim, A. J. Mäkinen, N. Nikolov, R. Shashidhar, H. Kim, Z. H. Kafafi, *Appl. Phys. Lett.* **2002**, *80*, 3844.
[18] X. Crispin, F. L. E. Jakobsson, A. Crispin, P. C. M. Grim, P. Anderson, A. Volodin, C. van Haesendonck, M. Van der Auweraer, W. R. Salaneck, M. Berggren, *Chem. Mater.* **2006**, *18*, 4354.
[19] J. Ouyang, Y. Yang, *Adv. Mater.* **2006**, *18*, 2141.
[20] B. Yoo, A. Dodabalapur, D. C. Lee, T. Hanrath, B. A. Korgel, *Appl. Phys. Lett.* **2007**, *90*, 072106.
[21] B. Chen, T. Cui, Y. Liu, K. Varahramyan, *Solid-State Electron.* **2003**, *47*, 841.
[22] J. Ouyang, C.-W. Chu, F.-C. Chen, Q. Xu, Y. Yang, *Adv. Funct. Mater.* **2005**, *15*, 203.
[23] S. K. M. Jönsson, J. Birgerson, X. Crispin, G. Greczynski, W. Osikowicz, A. W. Denier van der Gon, W. R. Salaneck, M. Fahlman, *Synth. Met.* **2003**, *139*, 1.
[24] S. Timpanaro, M. Kemerink, F. J. Touwslager, M. M. de Kok, S. Schrader, *Chem. Phys. Lett.* **2004**, *394*, 339–343.
[25] S. K. M. Jönsson, W. R. Salaneck, M. Fahlman, *J. Electron Spectrosc, Relat. Phenom.* **2004**, *137–140*, 805–809.
[26] J. Huang, P. F. Miller, J. S. Wilson, A. J. de Mello, J. C. de Mello, D. D. C. Bradley, *Adv. Funct. Mater.* **2005**, *15*, 290.
[27] V. K. S. Shante, C. M. Varma, A. N. Bloch, *Phys. Rev. B* **1973**, *8*, 4885.
[28] P. Sheng, B. Abeles, Y. Arie, *Phys. Rev. Lett.* **1973**, *3*, 44.
[29] P. Sheng, *Phys. Rev. B* **1980**, *21*, 2180.
[30] L. Zuppiroli, M. N. Bussac, S. Paschen, O. Chauvet, L. Forro, *Phys. Rev. B* **1994**, *50*, 5196.
[31] J. Ouyang, Q. Xu, C. W. Chu, Y. Yang, G. Li, J. Shinar, *Polymer* **2004**, *45*, 8443.
[32] S. Ashizawa, R. Horikawa, H. Okuzaki, *Synth. Met.* **2005**, *153*, 5.
[33] X. Crispin, S. Marciniak, W. Osikowicz, G. Zotti, A. W. Denier van der Gon, F. Louwet, M. Fahlman, L. Groenendaal, F. de Schryver, W. R. Salaneck, *J. Polym. Sci B* **2003**, *41*, 2561.
[34] A. M. Nardes, M. Kemerink, R. A. J. Janssen, *Phys. Rev. B.* **2007**, *76*, 085208.
[35] A. M. Nardes, M. Kemerink, R. A. J. Janssen, J. A. M. Bastiaansen, N. M. M. Kiggen, B. M. W. Langeveld, A. J. J. M. van Breemen, M. M. de Kok, *Adv. Mater.* **2007**, *19*, 1196.
[36] R. M. Hill, *Philos. Mag.* **1971**, *24*, 1307.
[37] M. Pollak, I. Riess, *J. Phys. C* **1976**, *9*, 2339.
[38] M. M. Fogler, S. Teber, B. I. Shklovskii, *Phys. Rev. B* **2004**, *69*, 035413.
[39] S. Samitsu, T. Shimomura, K. Ito, M. Fujimori, S. Heike, T. Hashizume, *Appl. Phys. Lett.* **2005**, *86*, 233103.
[40] A possible anisotropy in conductivity was not explicitly investigated, but the excellent sample-to-sample reproducibility suggests that if macroscopic anisotropy is present, its net magnitude is very small.
[41] J. Zhang, B. I. Shklovskii, *Phys. Rev. B* **2004**, *70*, 115317.